


ORIGINAL ARTICLE

Open Access



# SWATH-MS insights on sodium butyrate effect on mAbs production and redox homeostasis in CHO cells

Mauro Galli<sup>1</sup>, Lillian Chia-Yi Liu<sup>1</sup>, Kae Hwan Sim<sup>1</sup>, Yee Jiun Kok<sup>1</sup>, Katherine Wongtrakul-Kish<sup>1</sup>, Terry Nguyen-Khuong<sup>1</sup>, Stephen Tate<sup>2</sup> and Xuezhi Bi<sup>1,3,4\*</sup> 

## Abstract

Sodium butyrate (NaBu), well-known as a histone deacetylase inhibitor and for its capacity to impede cell growth, can enhance the production of a specific protein, such as an antibody, in recombinant Chinese hamster ovary (CHO) cell cultures. In this study, two CHO cell lines, namely K1 and DG44, along with their corresponding mAb-producing lines, K1-Pr and DG44-Pr, were cultivated with or without NaBu. A SWATH-based profiling method was employed to analyze the proteome. Cells cultured in the presence of NaBu exhibited a reduction in mitosis and gene expression, supported by their culture data demonstrating growth inhibition. The presence of NaBu corresponded to upregulation of intracellular trafficking and secretion pathways, aligned with an observed increase in mAb production, and was associated with an elevated glycosylation pathway and a slight alteration in the glycosylation profile of the mAbs. Increased fatty acid oxidation, redox interactions, and lipid biosynthesis were also observed and are likely attributable to the metabolism of NaBu. A comprehensive understanding of the systemic effects of NaBu will facilitate the discovery of strategies to enhance or prolong the productivity of CHO cells.

**Keywords** Butyric acid, CHO cells, SWATH-MS, Redox, mAbs

## Introduction

Biologics are rapidly growing in market share with the sales of biologics expected to be dominant (Senior 2023). To improve the development and production processes, a lot of efforts are dedicated to the implementation of quality by design approach, leading to safer and more effective products of higher quality (Newcombe 2014; Ortiz-Enriquez et al. 2016; Rizzo et al. 2022). Recombinant monoclonal antibodies (mAbs) covered 36% of the recombinant biopharmaceutical proteins in 2021 and over 70% of those are produced in CHO cells (Lalonde

and Durocher 2017). CHO cells produce high yields of recombinant proteins necessary for large-scale biopharmaceuticals manufacturing and are able to mimic human glycans in the production of glycoproteins (Lai et al. 2013).

Various research has been performed to increase the yield of CHO cells producing recombinant proteins, spanning from cell line engineering to treatment with specific compound (Lai et al. 2013). One of the molecules positively influencing CHO productivity is sodium butyrate (NaBu), the sodium salt of butyric acid. NaBu is known for its capacity to inhibit cell growth by arresting the cell cycle at the G0/G1 phase, thereby increasing the specific productivity of CHO cells which is reciprocal to cell growth and resulting in a rise of recombinant protein production. This is achieved by altering transcriptional regulation of certain genes through histone

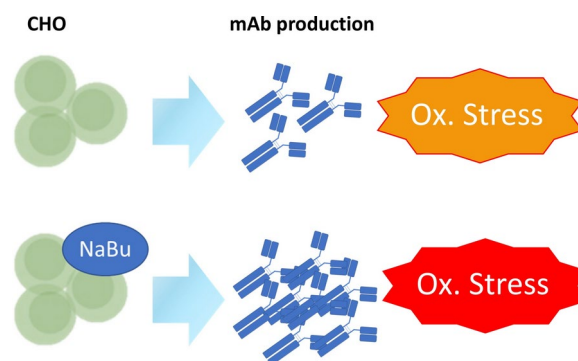
\*Correspondence:

Xuezhi Bi  
bi\_xuezhi@bti.a-star.edu.sg

Full list of author information is available at the end of the article



© The Author(s) 2024. **Open Access** This article is licensed under a Creative Commons Attribution-NonCommercial-NoDerivatives 4.0 International License, which permits any non-commercial use, sharing, distribution and reproduction in any medium or format, as long as you give appropriate credit to the original author(s) and the source, provide a link to the Creative Commons licence, and indicate if you modified the licensed material. You do not have permission under this licence to share adapted material derived from this article or parts of it. The images or other third party material in this article are included in the article's Creative Commons licence, unless indicated otherwise in a credit line to the material. If material is not included in the article's Creative Commons licence and your intended use is not permitted by statutory regulation or exceeds the permitted use, you will need to obtain permission directly from the copyright holder. To view a copy of this licence, visit <http://creativecommons.org/licenses/by-nc-nd/4.0/>.

**Graphical Abstract**

hyperacetylation (Davie 2003) as NaBu is a non-competitive inhibitor of class 1 and 2 histone deacetylases. However, NaBu also binds to pro-apoptotic proteins, leading to an activation of the apoptotic signals in CHO (Li et al. 2022) and multiple cancer cells (Hague et al. 1993; Jiang et al. 2012; Salimi et al. 2017). While a pro-autophagic effect was discovered, this was proposed as a pro-survival effect rather than a cell death mechanism of NaBu-treated cells to eliminate dysfunctional mitochondria (Lee and Lee 2012). A combination of NaBu treatment with apoptosis inhibitors as an attempt to mitigate the deleterious effects succeeded in promoting higher transgene expression compared to NaBu treatment alone (Li et al. 2022).

In an effort to improve the development and production pipeline in bioprocessing, we believe that a comprehensive omics-based systemic analysis of the effects of NaBu on CHO cells may facilitate greater understanding of its mechanism of action and open the path to further improvement in CHO production yield. Untargeted proteomics performed with sequential window acquisition of all theoretical mass spectra by mass spectrometry (SWATH-MS)– a data-independent acquisition (DIA) method– offers the chance to see thousands of proteins contemporaneously, allowing us to take a panoramic picture of the biology of the cells (Schubert et al. 2015; Ludwig et al. 2018). Subsequent pathway analyzes can identify essential leads towards higher NaBu-induced productivity, and reduce research and development time (Walker et al. 2017; Park et al. 2021). DIA-MS analysis is limited by the availability of a good quality spectral library, which is dependent on comprehensive data dependent acquisition and laborious curation. To support the application of DIA-MS for future research into recombinant biotherapeutic proteins production, our group has previously prepared extensive spectral libraries for CHO proteome and harvested cell culture fluid (Sim et al. 2020). In recent years, DIA-MS has been increasingly applied in bioprocess research to facilitate more

efficient processes and production of safer biotherapeutics (Walker et al. 2017; Orellana et al. 2017; López-Pedrouso et al. 2021). In this paper DIA was used to understand the double effect of NaBu on mAb-producing CHO cells, on one side it promotes an increased yield of production and on the other it contributes to an accumulation of oxidative stress, leading to apoptosis.

**Material and methods****Reagents and material**

Parental cell line CHO-K1 and CHO-DG44 were purchased from Merck (SAFC, Hub Carlsbad CA) and Thermo Fisher Scientific (Grand Island, NY) respectively. Sequencing-grade porcine trypsin was purchased from Promega Corporation (Madison, WI), and Rapid PNGase F from New England Biolabs (Ipswich, MA). Halt™ protease inhibitor cocktail and Pierce™ BCA Protein Assay Kit were purchased from Thermo Fisher Scientific (Waltham, MA); Glycoworks RapiFluor-MS *N*-glycan Kit, RFMS-labeled dextran and 50 mM ammonium formate solution were from Waters Corporation (Milford, MA); S-trap™ mini spin columns from ProtiFi™ (Huntington, NY). Acetonitrile (ACN) was from Merck (Burlington, MA), and all other reagents were purchased from Sigma-Aldrich (St Louis, MO, US) unless stated otherwise.

**Cell Culture**

All cell lines were cultured in a fully defined protein-free culture medium in 125 mL disposable Erlenmeyer shake flasks (Corning, Acton, MA) and incubated on a shaker platform at 110 rpm in a humidified 37 °C/8% CO<sub>2</sub> incubator. Viable cell density and viability were measured by Vi-CELL™ XR cell viability analyzer (Beckman Coulter, Brea, CA) as per manufacturer's instructions. The trastuzumab-producing CHO-K1 and CHO-DG44 cells, which were in-house generated stable cell lines by Dr. Yang Yuan Sheng (Cell Line Development group), were treated with or without 1 mM NaBu for 48 h and subjected to SWATH-MS analysis.

### Protein extraction and digestion

Cells were pelleted at  $1,500\times g$ , washed thrice with ice-cold phosphate-buffered saline (PBS) and resuspended in cell lysis buffer (5% sodium dodecyl sulfate (SDS), 50 mM triethylammonium bicarbonate buffer (TEAB), pH 8.5, and Halt™ protease inhibitor cocktail). Cell lysates were further disrupted using an ultrasonic processor (Model: UP50H, Hielscher Inc., Teltow, DE) at 100% amplitude with 0.5 s pulse on and 0.5 s pulse off for 20 times on ice and clarified by high-speed centrifugation at  $20,000\times g$  for 10 min. Protein concentration was determined using the Pierce™ BCA Protein Assay Kit according to manufacturer's instructions. Subsequently, 200 μg of protein from each sample was digested with 1:25 trypsin to protein ratio on S-trap™ mini spin columns (ProtiFi™, Huntington, NY) according to manufacturer's protocol, and peptide eluates were dried down using SpeedVac (Savant Instruments, Holbrook, NY).

### SWATH-MS data-independent acquisition

SWATH-MS acquisition was performed on nanoAcquity UPLC system (Waters) with ACQUITY UPLC M-class BEH C18 peptide column (75 μm internal diameter (i.d.) $\times$ 200 mm length, 1.7 μm particle size, 130 Å pore size) coupled to a TripleTOF 6600 mass spectrometer (SCIEX, Framingham, MA). Indexed retention time (iRT) peptides from Biognosys AG (Schlieren, CH) were added to all samples for retention time normalisation following manufacturer's instructions. The LC system was operated with buffer A (0.1% FA/water) and B (0.1% FA/ACN) at a flow rate of 300 nL/min. A two-step gradient (5–30/30–40% B) was performed over 106 min. The acquisition was performed with a 100-variable window scheme generated with the SWATH Variable Window Calculator 1.0 (SCIEX). An overlap of 1  $m/z$  was set at the lower limit of each window. The MS1 scan range covered 400–1,250  $m/z$  for 250 ms and MS2 spectra were acquired in high-sensitivity mode from 50 to 2,000  $m/z$  for 30 ms, resulting in a total cycle time of 3.3 s. To maintain the similarity between data-dependent acquisition (DDA) and DIA, the collision energy (CE) equation was conserved ( $0.0625\times m/z-10.5$ ) (Sim et al. 2020). The CE of a doubly charged precursor centered in the middle of the isolation window was applied to all the charge states, with a collision energy spread (CES) of 5 eV.

### In-gel trypsin digest and glycan release

In-gel trypsin digestion of excised SDS-PAGE separated gel bands containing mAb protein was performed as previously described (Chng et al. 2015) and extracted peptides were evaporated to dryness in a SpeedVac. Glycans were released and labeled using GlycoWorks RapiFluor-MS *N*-glycan Kit according to manufacturer's instructions. Peptides were re-solubilized in water

and GlycoWorks Rapid Buffer and incubation with 1.2 μL Rapid PNGase F at 50 °C for 10 min. RapiFluor-MS (RFMS) labeling solution was added to cooled samples and left at room temperature for 5 min. Samples were cleaned using a GlycoWorks HILIC μElution Plate and reconstituted in 25% dimethylformamide (DMF)/52.5% ACN (v/v) in water.

### HILIC-UPLC-FLR with ESI-MS

RFMS-labeled glycans were analyzed by HILIC-UPLC-FLR ESI-MS using a Waters ACQUITY UPLC H-Class coupled online to a Waters Xevo G2-S Q-TOF controlled by UNIFI Scientific Information System. RFMS-labeled glycans were injected onto an ACQUITY UPLC® Glycan BEH Amide Column (130 Å, 1.7 μm, 2.1 mm $\times$ 150 mm) at a flow rate of 0.4 mL/min and column temperature of 60 °C. Buffer A was 50 mM ammonium formate (pH 4.4) and Buffer B was 100% ACN. After an initial column equilibration of 2 min, glycans were separated using a linear gradient of 20%–49% of Buffer A for 40 min, increasing to 100% over 1.5 min, followed by 3 min washing. Fluorescence detection was used for glycan quantitation (Ex 265 nm/ Em 425 nm). For MS detection, samples were analyzed in sensitivity mode and spectra were acquired in positive ion mode with a full MS scan over a range of 400–2000  $m/z$  and accumulation time of 1 s. The instrument conditions were as follows: 2.75 kV electrospray ionisation capillary voltage, 15 V sample cone voltage, 120 °C ion source temperature, 300 °C desolvation temperature and 800 L/h desolvation gas flow.

### Construction of CHO global spectral library

Previously published DDA data (Sim et al. 2020) were submitted for database searches via Spectronaut v17 (Biognosys). The spectra were searched against *Cricetulus griseus* proteome from UniProt (UP000001075\_10029, 1 sequence per protein (1SPP), updated at 28–11-2022) containing 23,883 entries. 60 DDA WIFF files from wild-type CHO cells were searched to create an ion library using the Pulsar engine. Peptide, protein, and peptide-spectrum match (PSM) false discovery rates (FDR) were set at 1%. Fragment ions  $m/z$  range was set between 100 and 1800, precursors were selected with a minimum of 3 and a maximum of 6 fragments per peptide. A maximum of 2 missed cleavages was permitted.

### Data analysis

SWATH analysis was accomplished using Spectronaut 17 (Biognosys). The DIA spectra data were searched against the CHO global spectral library followed by *C. griseus* database (UniProt UP000001075\_10029 1SPP). For identification, the precursor  $q$ -value cutoff was set at 0.01 and posterior error probability (PEP) was set to 0.2. The protein  $q$ -value cutoff at the experiment level was set at

0.01 and at the run level at 0.05. The run-wise PEP was set at 0.75. For quantitation, only precursors identified in at least 20% of the runs were retained with background signal selected as the imputation strategy for missing values. Differentially abundant candidates were tested with an unpaired t-test assuming equal variance, and a group-wise multiple testing correction was applied. The candidates were filtered for Absolute AVG Log2Ratio > 0.58,  $q$ -value < 0.05 and Unique Peptides > 2. Subsequent pathway analysis was performed using Cytoscape and its collection of applications: stringApp, EnrichmentMap and AutoAnnotate (Shannon et al., 2003).

The upregulated and downregulated candidates were analyzed separately for each condition of interest. The list of the differentially regulated proteins was queried in String with 0.4 confidence score cut-off against the *C. griseus* organism database. A network of enriched proteins was retrieved from String and a subnetwork was created with the core enriched proteins. Log2FC and  $q$ -values were imported in the node tables to visualize up- and downregulated proteins in the pathways. A String Enrichment analysis was performed on the subnetwork. The enrichment results were filtered for Gene Ontology (GO) processes and redundant terms were removed. The enrichment maps were calculated based on String Enrichment analysis, with similarity score cutoff set at 0.4 for downregulation and at 0.3 for upregulation. AvgLog2ratio was imported in the enrichment map. The AutoAnnotation app was used on the enrichment map to highlight the groups. The groups of interest were isolated for further functional GO processes terms enrichment analysis.

#### Data availability

The data that support the findings of this study are available on PRIDE with the following identifier PXD048575.

## Results

### NaBu's effect on cell viability, growth, and mAb production

The effects of NaBu on CHO cells at a systemic level were studied by SWATH-MS-based untargeted analysis of the proteomes of two CHO cell lines, K1 and DG44: both untransfected parental (Pa) and mAb-producing (Pr) cells were cultured with or without NaBu supplementation. The viability of all cell lines assayed at 0, 24 and 48 h in culture was similar (Fig. 1B, E), but NaBu-treated cells were increasing at a slower rate at 24 h and 48 h compared to untreated control cells (Fig. 1A, D). These observations corroborated NaBu's known function as a growth inhibitor (Davie 2003). NaBu is also known to enhance the synthesis of recombinant proteins (Han et al. 2005; Lee and Lee 2012; Hong et al. 2014), and this was reflected in NaBu-treated cells having augmented yield and titer compared to the control cells (Fig. 1C,

F). A more marked effect upon NaBu treatment was observed in DG44-Pr compared to K1-Pr, with ~90% increase in specific productivity in DG44-Pr and ~57% in K1-Pr. The ability of NaBu to inhibit DNA replication and cell growth in CHO cells, and thereby increasing cellular resources for the synthesis of recombinant proteins was also shown by other groups (Hua et al. 2022). Furthermore, other means of arresting CHO cells in G0/G1 phases were also demonstrated to influence protein synthesis and increase recombinant protein production in CHO cells. Lu et al. (2023) showed the efficacy of apilimod in blocking the cell cycle in G0/G1 to favour protein production, while Lataster et al. (2023) promoted protein production by blocking the cells in G0/G1 using an optogenetic approach to influence p21, a cell cycle inhibitor. An additional confirmation of the improved productivity of CHO cells in G0/G1 phase was given by the work of Dutton et al. (2006). The positive link between G0/G1 cell cycle phase and productivity may also explain in part the larger increase in specific productivity observed in DG44-Pr compared to K1-Pr cells upon NaBu treatment, as we have previously detected lower expression of cell-cycle progression genes and proteins (and hence greater sensitivity to the disruptive effect of NaBu on cell replication) in DG44 cell line (Lakshmanan et al. 2019).

### PCA and analysis workflow

SWATH data analysis was performed using Spectronaut 17 and a CHO ion library of 9,367 proteins generated by reprocessing data previously acquired at our laboratory by Sim et al. (2020) (Fig. 2A). Analysis of all samples yielded 6,145 (95.1%) of quantifiable proteins at a  $q$ -value cutoff of 0.01 (Fig. 2B). Principal component analysis (PCA) in Fig. 2C showed distinct clustering for each sample, with cell lineage primarily contributing to variation in PC1 (30.65%), NaBu treatment in PC2 (18.80%) and mAb production in PC3 (8.78%), and a total variance of 58.23% explained by the three PCs. Differentially expressed proteins between untreated control and NaBu-treated cells were subsequently subjected to pathway analysis using Cytoscape (Fig. 2A). Similar pathways were being affected following NaBu treatment in the parental (Suppl. Table S1 and S2) and their corresponding mAb-producing cells (Figs. 3 and 4), with the latter showing more marked changes and thus focused upon to illustrate the effects of NaBu treatment in K1 and DG44 cell lines.

### NaBu upregulated pathways and areas

NaBu treatment in mAb-producing cells upregulated pathways which converged in three macro-areas: metabolism, intracellular trafficking, and oxidation–reduction (redox) (Table 1, Fig. 3). Within metabolism, the more pronounced changes were observed in lipid metabolism and fatty acids oxidation for both the producing cell

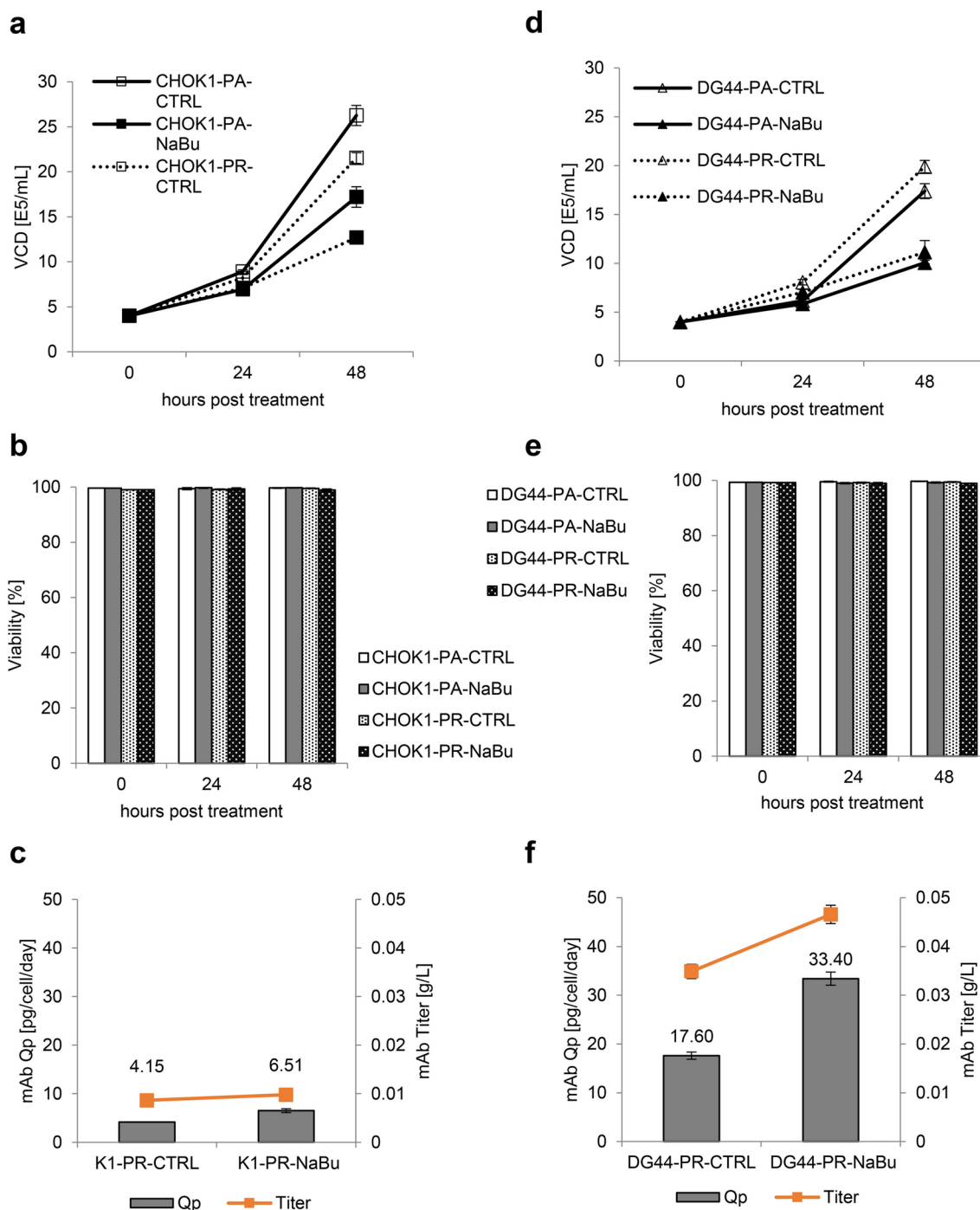


**Fig. 1** Cell culture viability and yield. The effects of sodium butyrate (NaBu) on **A,D** viable cell density, **B,E** viability and **C,F** mAb production yield in CHO-K1 and CHO-DG44 parental and production cells. Viable cell density and viability were analyzed by trypan blue exclusion and measured at day 0, 1 and 2 after inoculation. The titer (g/L) and specific productivity (pg/cell/day) were determined by ELISA assay. All error bars showed the standard deviation of three biological replicates

lines. DG44-Pr hits a higher number of GO processes and proteins compared to K1-Pr. The lipid and ion transport cluster suggests increased lipid movements in or across the cells under the influence of NaBu. Other metabolic pathways were also upregulated in DG44-Pr under NaBu. K1-Pr shows a distinct cluster of upregulation of

glycoprotein biosynthesis, in accordance with increased mAb production shown in Fig. 1C. The positively regulated *N*-linked glycosylation pathway of K1-Pr was shown in Suppl. Fig. S1A. The same pathway was statistically filtered out in DG44-Pr, but the most upregulated protein (phosphomannomutase—G3IJJ7) was upregulated

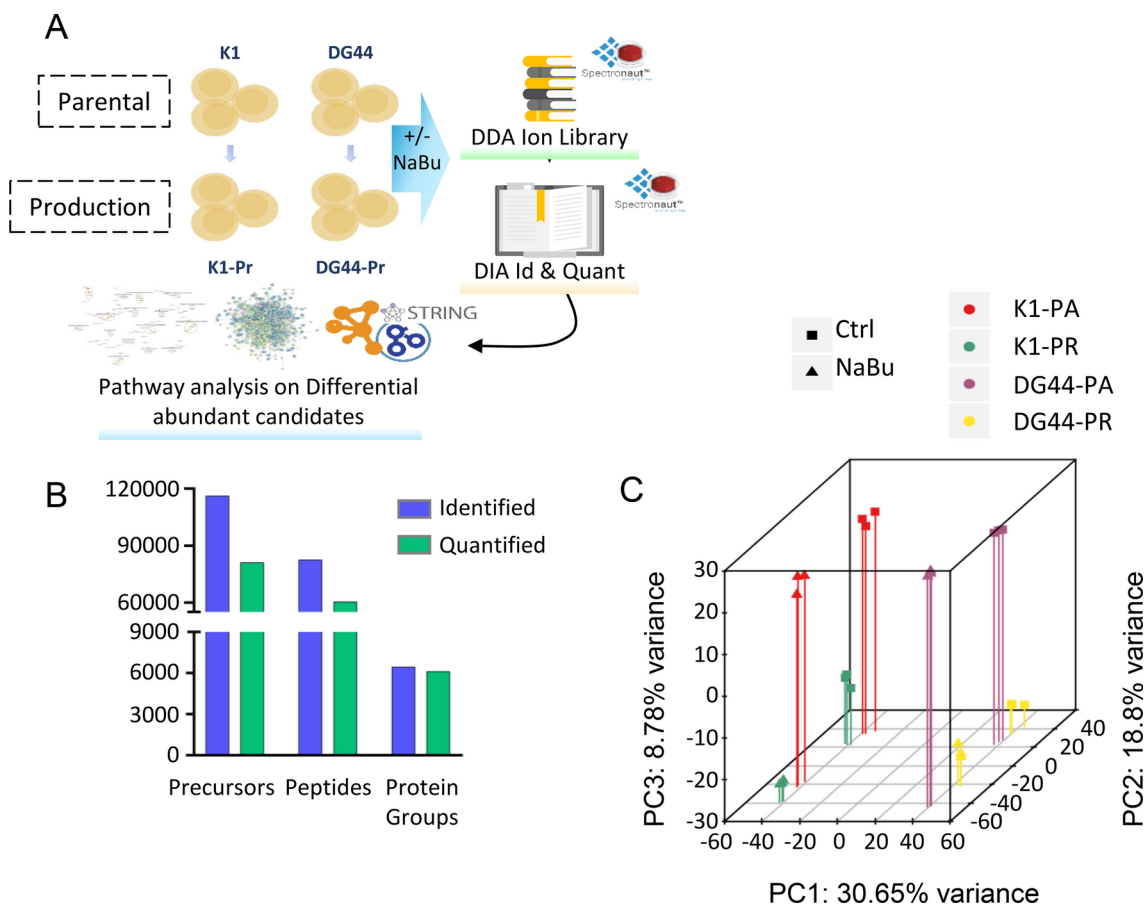


**Fig. 2** CHO Treatment and SWATH analysis. **A** Parental (K1-Pa and DG44-Pa) and production (K1-Pr and DG44-Pr) CHO cell lines untreated or treated with NaBu. 60 CHO global library DDA runs were reprocessed with Spectronaut 17 to create the ion library. CHO SWATH runs were analyzed in Spectronaut 17 and differentially abundant candidates were selected. A pathways regulation analysis was performed using String and Gene ontology through Cytoscape. **B** Precursors, peptides and proteins identified at 0.01  $q$ -value (Blue) and quantified (Green). **C**: 3D principal component analysis (PCA) of the runs calculated by PCAGO (<https://github.com/rumangerst/pcago-unified>) (Holzer, 2019). Component 1 covers 30.65% of variance, component 2 the 18.8% and component 3 the 8.78%, explaining the 58.23% of the total variance

in both the cell lines. Several studies have shown that the addition of NaBu in cell culture resulted in the alteration of glycosylation on therapeutic proteins (Rodriguez et al. 2005; Cabrera et al. 2005; Hong et al. 2014). A typical  $N$ -glycan profile was shown here with a high percentage of bi-antennary glycans and core fucosylation in the mAbs produced from K1-Pr and DG44-Pr cells (Suppl. Fig. S1B, C). Upon NaBu treatment, the  $N$ -glycan profile of mAbs showed slightly higher galactosylation and lower fucosylation compared to the products from untreated cultures (Suppl. Fig. S1D, E). Nevertheless, the overall pattern of glycosylation remained similar in the presence or absence of NaBu. Finally, glycoside metabolism and ribonucleoside bisphosphate metabolism clusters were upregulated in K1-Pr, with the main process of the latter upregulated in DG44-Pr too.

Intracellular trafficking is supported by many interconnected GO processes grouping for the common features of signaling and intracellular trafficking. This

result agreed with Fig. 1C, highlighting increased secretory activity from augmented mAb production. At the same time, it revealed the possible effects of autophagy as well, evidenced by increased vacuole mobilization in the cells. Increased production of mAb and metabolic activities by the treatment promoted multiplication of redox exchanges inside the cells, especially those involving the endoplasmic reticulum (ER) and mitochondria (Ha et al. 2018). The redox cluster showed activation of the response mechanism to stresses in the cells for both nitrogenous compounds and hydrogen peroxide. The enrichment of the single GO processes with their FDR values for both DG44-Pr and K1-Pr is reported in Table 1.

#### NaBu downregulated pathways and areas

NaBu was not only inducing an upregulation of several pathways, but also a downregulation of other pathways, as shown in Fig. 4. The main downregulatory effects of

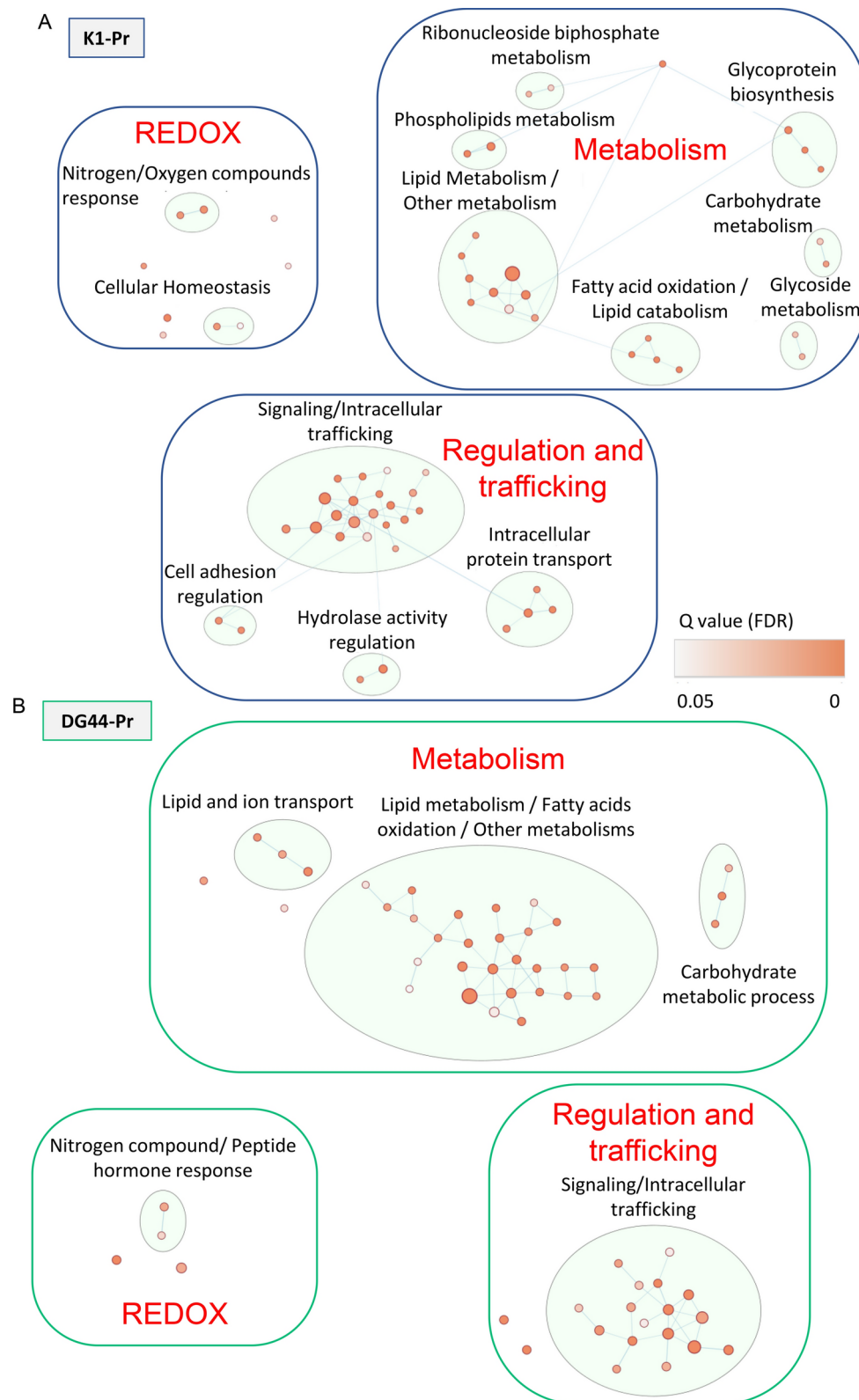


**Fig. 3** NaBu upregulated Lipid metabolism, REDOX exchanges and Signalling/Intracellular trafficking in CHO cells. Differentially upregulated abundant proteins were imported into Cytoscape. A network was retrieved through the StringApp and a String functional enrichment was performed. An enrichment map was created using the Enrichment Map app on the enriched GO biological processes. Clusters of interest are reported for **A** K1-Pr and for **B** DG44-Pr. The dimension of the nodes is determined by the number of the proteins representing the process and the color represents the  $q$ -value (FDR). The node cutoff was set at  $q$ -value 0.05 and the similarity cutoff (Edge cutoff) was set at 0.3. Nodes details are reported in Table 1 and 2

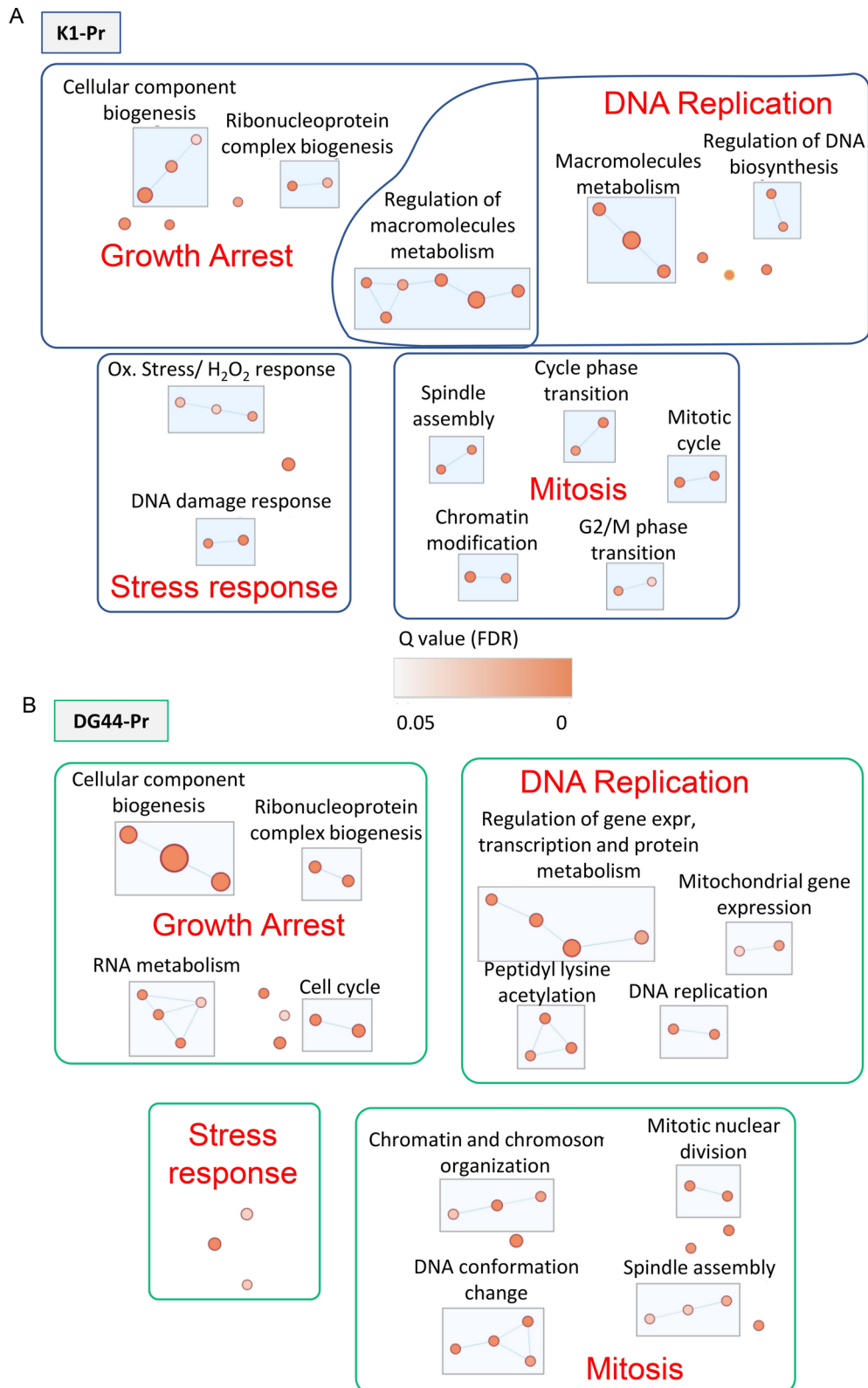


**Fig. 4** NaBu induced inhibition of gene expression, cell cycle, mitosis and gene expression-related stress response in CHO cells. Differentially downregulated proteins were imported into Cytoscape. A network was retrieved through the StringApp and a String functional enrichment was performed. An enrichment map was created on the enriched GO biological processes. Clusters of interest are reported for **A** K1-Pr and for **B** DG44-Pr. The dimension of the nodes is determined by the number of the proteins representing the process and the color represents the  $q$ -value (FDR). The node cutoff was set at  $q$ -value 0.05 and the similarity cutoff (Edge cutoff) was set at 0.4. Nodes details are reported in Table 3 and 4



**Table 1** Upregulated pathways in NaBu-treated CHO K1-Pr cells

<b>K1-Pr</b>					
<b>Primary area</b>	<b>Cluster</b>	<b>GO process</b>	<b>Description</b>	<b>FDR q-value</b>	<b>Protein number</b>
Metabolism	Lipid Me- tabolism / Other metabolism	GO:0044281	Small molecule metabolic process	1.9E-15	121
		GO:0008152	Metabolic process	9.8E-12	365
		GO:0006629	Lipid metabolic process	1.1E-07	79
		GO:0009058	Biosynthetic process	6.3E-07	131
		GO:0032787	Monocarboxylic acid metabolic process	6.7E-05	39
		GO:0008610	Lipid biosynthetic process	7.2E-04	34
		GO:0044283	Small molecule biosynthetic process	7.3E-03	33
		GO:1,901,362	Organic cyclic compound biosynthetic process	1.1E-02	51
		GO:1,901,360	Organic cyclic compound metabolic process	3.9E-02	121
		Fatty acid oxidation / Lipid catabolism	GO:0044242	Cellular lipid catabolic process	1.3E-04
	GO:0006520		Cellular amino acid metabolic process	5.3E-04	24
	GO:0046395		Carboxylic acid catabolic process	5.3E-04	22
	Glycoprotein Biosynthesis	GO:0019395	Fatty acid oxidation	5.4E-03	11
		GO:1,901,135	Carbohydrate derivative metabolic process	1.5E-09	72
		GO:0009101	Glycoprotein biosynthetic process	1.1E-05	30
	Phospholipids Metabolism	GO:0006487	Protein n-linked glycosylation	6.0E-04	12
		GO:0006793	Phosphorus metabolic process	1.1E-05	104
	Carbohydrate metabolism	GO:0019637	Organophosphate metabolic process	1.9E-04	51
		GO:0019318	Hexose metabolic process	9.6E-03	14
	Glycoside metabolism	GO:0005975	Carbohydrate metabolic process	2.9E-02	29
		GO:1,901,657	Glycosyl compound metabolic process	1.9E-02	12
	Ribonucleoside biphosphate metabolism	GO:0016137	Glycoside metabolic process	2.6E-02	5
		GO:0015936	Coenzyme a metabolic process	2.0E-02	5
	Individual nodes of interest	GO:0033875	Ribonucleoside bisphosphate metabolic process	3.2E-02	11
		GO:0055086	Nucleobase-containing small molecule metabolic process	3.6E-04	35

**Table 1** (continued)

K1-Pr							
Primary area	Cluster	GO process	Description	FDR <i>q</i> -value	Protein number		
Regulation and trafficking	Signaling / Intracellular trafficking	GO:0051179	Localization	1.5E-09	242		
		GO:0032879	Regulation of localization	8.0E-07	147		
		GO:0065008	Regulation of biological quality	3.2E-06	185		
		GO:0016043	Cellular component organization	4.4E-06	233		
		GO:0060627	Regulation of vesicle-mediated transport	2.0E-04	42		
		GO:0010941	Regulation of cell death	2.1E-04	89		
		GO:0051128	Regulation of cellular component organization	5.3E-04	120		
		GO:0032880	Regulation of protein localization	6.6E-04	58		
		GO:0043065	Positive regulation of apoptotic process	8.6E-04	43		
		GO:0060341	Regulation of cellular localization	9.5E-04	62		
		GO:0051050	Positive regulation of transport	1.3E-03	57		
		GO:0048585	Negative regulation of response to stimulus	2.3E-03	80		
		GO:0022607	Cellular component assembly	4.2E-03	104		
		GO:0048522	Positive regulation of cellular process	6.1E-03	226		
		GO:0023051	Regulation of signaling	9.7E-03	140		
		GO:0080134	Regulation of response to stress	1.2E-02	64		
		GO:0030100	Regulation of endocytosis	1.5E-02	19		
		GO:0050727	Regulation of inflammatory response	2.9E-02	23		
		GO:0050793	Regulation of developmental process	3.6E-02	116		
		GO:1,903,530	Regulation of secretion by cell	4.4E-02	37		
		Intracellular protein transport		GO:0008104	Protein localization	4.5E-07	115
				GO:0006886	Intracellular protein transport	7.4E-04	51
				GO:0033365	Protein localization to organelle	4.3E-03	41
				GO:0016192	Vesicle-mediated transport	4.7E-03	67
		Cell adhesion regulation		GO:0030155	Regulation of cell adhesion	3.4E-03	44
				GO:0051270	Regulation of cellular component movement	4.2E-03	58
Hydrolase activity regulation		GO:0050790	Regulation of catalytic activity	1.1E-04	114		
		GO:0051345	Positive regulation of hydrolase activity	6.2E-03	42		
Redox	Nitrogen/Oxygen compounds response	GO:1,901,700	Response to oxygen-containing compound	4.2E-03	75		
		GO:1,901,698	Response to nitrogen compound	6.3E-03	55		
	Cellular homeostasis		GO:0019725	Cellular homeostasis	7.0E-03	48	
			GO:0070838	Divalent metal ion transport	4.6E-02	21	
	Individual nodes of interest		GO:0055114	Oxidation–reduction process	4.4E-06	67	
			GO:0036295	Cellular response to increased oxygen levels	8.3E-03	5	
			GO:2,001,233	Regulation of apoptotic signaling pathway	3.1E-02	26	
			GO:0010508	Positive regulation of autophagy	3.2E-02	13	
		GO:0045454	Cell redox homeostasis	4.0E-02	7		

The table describes in detail the areas influenced by NaBu in Fig. 3A. Clusters characterize the different areas, and each cluster is described by the GO processes supporting the upregulation. For each GO process the description, the number of the proteins and the FDR corrected *q*-value is reported

NaBu were clustered into four areas of potential interest: DNA replication, mitosis, growth arrest and stress response. Both cell lines shared the ribonucleoprotein complex biogenesis cluster, highlighting a common propensity of NaBu treatment to reduce the biosynthesis of constituent macromolecules for other cellular activities. This was complemented by a decrease in proteins involved in cellular component biogenesis for K1-Pr and in proteins important for the cell cycle in DG44-Pr. Taken together, they indicated a growth arrest of the NaBu-treated cells. While the apparent effect of NaBu

on treated CHO cells was an increase in mAb production, de facto, it was exerting its effect at the level of DNA replication (Lee and Lee 2012; Jiang et al. 2012; Li et al. 2022). In the analyzed cell lines, NaBu induced an inhibition of gene expression and mitotic mechanisms, hinting that the cells were stranded in the G1 phase (Fig. 4). Our pathway analysis confirms the known effects of NaBu on the cell cycle (Semaan et al. 2020; Avello et al. 2022). The arrest of the cell cycle is compatible with the effects seen on CHO cell viability and mAb production. High cell viability shown in Fig. 1 confirmed that the cells

were viable at the moment of the experiment; the lower number of cells compared to the control was due to the growth arrest as seen in the pathway analysis. The augmented mAb production may be due to increased availability of resources with the blocking of the cell cycle and the consequent redirection of cellular machinery for protein production. A similar behaviour was observed when the cell cycle was arrested by thymidine or NaBu (Al-Rubeai et al. 1992; Avello et al. 2022). The downregulation of the DNA replication was supported by DG44-Pr data, where different processes clustered in the peptidyl lysine acetylation group. The downregulation of this GO process corresponded to greater histone acetylation due to the inhibition of histone deacetylases, and increased acetylation of histones is known to alter DNA replication (Kruh 1981; Davie 2003). Western blot of control and NaBu-treated K1 and DG44 cells showed a marked increase in the acetylation of Histone H4 upon NaBu treatment (Suppl. Fig. S2), thus confirming the known effect of NaBu on cells and supporting the inhibition of DNA replication (Tables 2, 3 and 4).

From the results in both K1-Pr and DG44-Pr, a clear inhibition of mitotic activities in these CHO cells as a consequence of NaBu treatment was evidenced by multiple clusters of downregulated pathways (Fig. 4). Despite slight differences in the processes, there were 5 pathway clusters displaying a common behaviour. Pathways associated with mitotic nuclear division and chromatin and chromosome organisation/modification were inhibited in both cell lines upon NaBu treatment. Furthermore, diminished spindle assembly activity was reported for K1-Pr that could be coupled with actomyosin contractile ring inhibition. DG44-Pr exhibited diminished spindle assembly and heterochromatin formation, which is important for sister chromatid cohesion.

Stress response was the last downregulated macro area observed in NaBu-treated cells (Fig. 4). Two defined clusters denoting a minor response to DNA damage and a decreased response to oxidative stress/H<sub>2</sub>O<sub>2</sub> were observed in K1-Pr cells. No cluster was observed in DG44-Pr, but the trend of decreased stress response was maintained by the single processes.

## Discussion

This work aimed to decipher the systemic effects of NaBu on CHO cells. Understanding the problems arising from NaBu treatment can pave the road to new solutions, improving its beneficial effects or mitigating adverse outcomes from its administration to mAb-producing cells. Global proteome changes profiled by SWATH-MS, together with cell culture and product glycosylation data, were analyzed to obtain a systemic view of the pathways altered by NaBu in the cells. The spectral ion library was recompiled from previously acquired DDA runs (Sim et

al. 2020) using the latest version of Spectronaut Pulsar engine with enhanced capabilities to improve the library without lowering the quality of the data. While this global library, built from existing DDA data of fractionated wild type CHO cell samples, provided an extensive coverage of the CHO proteome and allowed for a fast analysis of the experiment, constructing a project specific library from samples including all the experimental conditions will likely have a higher statistical power and may lead to better results (Ludwig et al. 2018).

The known effects of NaBu, inhibition of cell proliferation and influence on histone modification, shown in this DIA-based proteomics study corroborated with the transcriptomic analysis by Schulze et al. (2022), the gene expression analysis by Wippermann et al. (2017) and the DDA proteomics analysis by Müller et al. (2017). The nature of NaBu, being a short-chained fatty acid (SCFA), has to be taken into consideration in the interpretation of the metabolic upregulation observed. A disproportion between fatty acid uptake and oxidation can lead to the accumulation of fatty acids and lipids in cytosol (van Eunen et al. 2013). An abundance of long-chained fatty acids is known to induce a lipid overload effect (Nguyen et al. 2008; Alsabeeh et al. 2018). Fatty acids are processed through the beta-oxidation cycle, and they can further undergo a de novo lipid biogenesis phase leading to the accumulation of lipid droplets or secretion of lipoproteins (Menendez and Lupu 2007; Walther and Farese 2012; van Eunen et al. 2013). These biological activities are implicated with an upregulation of mitochondrial activities and oxidative processes in the cells. The increased redox exchanges, another cluster that we found to be upregulated, commonly provoke the accumulation of oxidative stress and development of mitochondrial dysfunction (Nakamura et al. 2012; Wang et al. 2013; Ezquerro et al. 2020; Rios-Morales et al. 2022). The machineries connected with FA (FA oxidation and lipids synthesis) are upregulated in the analysis. As seen, it resulted in a natural increase in redox exchanges and oxidative stress accumulation. At the same time, the hyperactive protein synthesis machinery of the ER contributed to a further accumulation of oxidative stress, which is another source of future ER stress (Ozcan et al. 2004; Ha et al. 2018; Ezquerro et al. 2020; Gast et al. 2021). Cellular stress response machinery such as the production of glutathione are used to manage redox stress and working to keep the situation under tolerable limits.

The increased production of the recombinant protein seen in NaBu cells leads to increased secretion, resulting in additional stress for the secretory machinery (Lim et al. 2010). NaBu treatment is also known to induce autophagy activation in CHO cells (Lee and Lee 2012). The major metabolic activities, together with the boosted production of mAb, the response to oxidative stress and

**Table 2** Upregulated pathways in NaBu-treated CHO DG44-Pr cells

DG44-Pr					
Primary area	Cluster	GO process	Description	FDR q-value	Protein number
Metabolism	Lipid metabolism / Fatty acids oxidation / Other metabolisms	GO:0044281	Small molecule metabolic process	2.3E-15	98
		GO:0008152	Metabolic process	2.7E-10	273
		GO:0006629	Lipid metabolic process	8.7E-07	62
		GO:0009056	Catabolic process	1.3E-05	85
		GO:0044283	Small molecule biosynthetic process	1.7E-05	34
		GO:1,901,135	Carbohydrate derivative metabolic process	2.2E-05	48
		GO:0019752	Carboxylic acid metabolic process	2.8E-05	45
		GO:0044242	Cellular lipid catabolic process	1.6E-04	18
		GO:0009058	Biosynthetic process	2.2E-04	93
		GO:0019637	Organophosphate metabolic process	3.0E-04	41
		GO:0008610	Lipid biosynthetic process	3.2E-04	29
		GO:0044282	Small molecule catabolic process	3.2E-04	24
		GO:1,901,362	Organic cyclic compound biosynthetic process	6.4E-04	45
		GO:1,901,136	Carbohydrate derivative catabolic process	1.5E-03	14
		GO:1,901,615	Organic hydroxy compound metabolic process	2.0E-03	26
	GO:0006694	Steroid biosynthetic process	4.9E-03	11	
	GO:0072521	Purine-containing compound metabolic process	6.0E-03	21	
	GO:0006631	Fatty acid metabolic process	6.0E-03	21	
	GO:0016125	Sterol metabolic process	6.0E-03	12	
	GO:0046165	Alcohol biosynthetic process	7.1E-03	11	
	GO:0046434	Organophosphate catabolic process	1.1E-02	12	
	GO:0072523	Purine-containing compound catabolic process	1.9E-02	7	
	GO:0019395	Fatty acid oxidation	3.5E-02	8	
	GO:0046475	Glycerophospholipid catabolic process	4.0E-02	5	
	GO:1,901,360	Organic cyclic compound metabolic process	4.3E-02	92	
	GO:0033875	Ribonucleoside bisphosphate metabolic process	4.4E-02	9	
	GO:0015936	Coenzyme a metabolic process	4.8E-02	4	
	Carbohydrate meta- bolic process	GO:0005975	Carbohydrate metabolic process	3.8E-04	29
		GO:0044262	Cellular carbohydrate metabolic process	5.7E-03	14
		GO:0019318	Hexose metabolic process	2.3E-02	11
	Lipid and ion transport	GO:0006811	Ion transport	1.5E-03	56
		GO:0010876	Lipid localization	5.4E-03	22
		GO:0015711	Organic anion transport	1.3E-02	24
	Individual nodes of interest	GO:0016192	Vesicle-mediated transport	4.0E-04	57
		GO:0019216	Regulation of lipid metabolic process	1.1E-02	21
		GO:0045923	Positive regulation of fatty acid metabolic process	3.7E-02	6

**Table 2** (continued)

DG44-Pr					
Primary area	Cluster	GO process	Description	FDR <i>q</i> -value	Protein number
Regulation and trafficking	Signaling / Intracellular trafficking	GO:0051179	Localization	5.1E-11	193
		GO:0032879	Regulation of localization	1.2E-06	115
		GO:0008104	Protein localization	5.8E-06	87
		GO:0051128	Regulation of cellular component organization	2.0E-05	100
		GO:2,000,145	Regulation of cell motility	1.2E-04	49
		GO:0065008	Regulation of biological quality	2.2E-04	135
		GO:0010941	Regulation of cell death	7.5E-04	68
		GO:0050790	Regulation of catalytic activity	6.0E-03	81
		GO:0016043	Cellular component organization	1.1E-02	159
		GO:0060627	Regulation of vesicle-mediated transport	1.1E-02	29
		GO:0043065	Positive regulation of apoptotic process	1.3E-02	31
		GO:0048585	Negative regulation of response to stimulus	1.4E-02	59
		GO:0042592	Homeostatic process	1.8E-02	60
		GO:0051050	Positive regulation of transport	2.9E-02	40
		GO:0051345	Positive regulation of hydrolase activity	2.9E-02	31
		GO:0022603	Regulation of anatomical structure morphogenesis	4.4E-02	43
GO:0032880	Regulation of protein localization	4.4E-02	39		
	Individual nodes of interest	GO:0006928	Movement of cell or subcellular component	1.2E-03	60
Redox	Nitrogen compound / peptide hormone response	GO:1,901,698	Response to nitrogen compound	1.4E-02	42
		GO:0043434	Response to peptide hormone	3.4E-02	19
		GO:0055114	Oxidation–reduction process	3.5E-10	65
		GO:0006950	Response to stress	1.5E-02	103

The table describes in detail the areas influenced by NaBu in Fig. 3B. Clusters characterize the different areas, and each cluster is described by the GO processes supporting the upregulation. For each GO process the description, the number of the proteins and the FDR corrected *q*-value is reported

the activation of autophagy are all mechanisms behind the upregulation of the intracellular signaling and trafficking, the third positively modulated area highlighted during the analysis. The downside of NaBu treatment was that its inhibitory effects seemed to impair the ability of the cells to activate an important response mechanism such as the redox stress one. On the contrary, it has been reported that NaBu activates Nrf2 (Dong et al. 2017), a transcription factor activated by the increase of oxidative stress in the cytoplasm leading to antioxidant response (Bryan et al. 2013). The activation was seen in mice experiments and not in cell culturing experiments as in our case, where we found a downregulation of proteins connected with the antioxidant response. This downregulation is a major problem, considering NaBu itself is expected to be an indirect source of oxidative stress. Based on previous studies and our results, we propose a working model for the effects of NaBu on mAb-producing cells and potential mitigations that can be taken to prolong production time and yield (Fig. 5). The partial response of cells to redox stress impairs their ability to control oxidative stress accumulation, promoted by increased burden on mitochondrial respiratory machinery and fatty acids beta-oxidation. The ER, which is one

of the responsible for buffering oxidative stress, may not be available to manage the escalation in redox activity with it being consigned for mAb synthesis. This may intensify ER stress and further oxidative stress accumulation (Ha et al. 2018). In this situation, the antioxidant response should be activated at capacity, but its partial reaction due to NaBu treatment hampers the ability of the cells to control the oxidative stress levels. These complicated circumstances likely push the cells to activate their apoptotic and autophagic mechanisms, starting the processes that will eventually lead to cell death (Fig. 5). Hypothetically, an attempt to control NaBu-induced oxidative stress accumulation in these cells may prevent the onset of early apoptosis and allow longer production times. Our conclusion would explain the optimal results obtained on CHO culturing in bioreactors by Han et al. (2005). With the addition of the antioxidant N-acetylcysteine, they managed to prolong the culture for almost 200 h, doubling the production yield compared to cells solely treated with NaBu.

**Table 3** Downregulated pathways in NaBu-treated CHO K1-Pr cells

K1-Pr					
Primary area	Cluster	GO process	Description	FDR <i>q</i> -value	Protein number
Growth arrest	Cellular component biogenesis	GO:0071840	Cellular component organization or biogenesis	9.4E-05	170
		GO:0044085	Cellular component biogenesis	8.6E-03	82
		GO:0034622	Cellular protein-containing complex assembly	3.4E-02	33
	Ribonucleoprotein complex biogenesis	GO:0034470	ncRNA processing	2.2E-04	26
		GO:0022613	Ribonucleoprotein complex biogenesis	2.1E-02	24
	Regulation of macromolecules metabolism	GO:0060255	Regulation of macromolecule metabolic process	7.0E-10	213
		GO:0051246	Regulation of protein metabolic process	1.3E-04	102
		GO:0010605	Negative regulation of macromolecule metabolic process	1.4E-04	100
		GO:0051338	Regulation of transferase activity	8.9E-04	44
		GO:0044093	Positive regulation of molecular function	2.0E-03	65
	Individual nodes of interest	GO:0031401	Positive regulation of protein modification process	1.2E-02	48
		GO:0051301	Cell division	1.9E-03	29
		GO:0009058	Biosynthetic process	3.3E-03	83
GO:0033044		Regulation of chromosome organization	1.1E-02	21	
DNA replication	Macromolecules metabolism	GO:0043170	Macromolecule metabolic process	2.2E-21	240
		GO:0090304	Nucleic acid metabolic process	6.3E-16	110
	Regulation of DNA biosynthesis	GO:0006464	Cellular protein modification process	9.0E-08	112
		GO:0051052	Regulation of DNA metabolic process	2.0E-03	23
		GO:2,000,278	Regulation of DNA biosynthetic process	7.4E-03	11
	Individual nodes of interest	GO:0006397	mRNA processing	2.9E-06	33
		GO:0006259	DNA metabolic process	2.2E-05	40
Mitosis	Chromatin modification	GO:0009057	Macromolecule catabolic process	9.1E-04	42
		GO:0051276	Chromosome organization	1.9E-06	
	Spindle assembly	GO:0016569	Covalent chromatin modification	3.5E-03	
		GO:1,902,850	Microtubule cytoskeleton organization involved in mitosis	1.3E-03	
	Mitotic cycle	GO:0051225	Spindle assembly	3.5E-03	56
		GO:0000278	Mitotic cell cycle	4.8E-06	23
		GO:0140014	Mitotic nuclear division	3.1E-05	12
		GO:0010564	Regulation of cell cycle process	5.1E-05	10
	Cycle phase transition	GO:1,901,990	Regulation of mitotic cell cycle phase transition	8.3E-03	36
		GO:1,902,749	Regulation of cell cycle G2/M phase transition	1.1E-02	17
Stress response	Ox. stress / H <sub>2</sub> O <sub>2</sub> response	GO:0072425	Signal transduction involved in G2 DNA damage checkpoint	3.3E-02	36
		GO:0006979	Response to oxidative stress	1.1E-02	17
		GO:0010035	Response to inorganic substance	2.5E-02	10
	DNA damage response	GO:0042542	Response to hydrogen peroxide	3.2E-02	4
		GO:0080135	Regulation of cellular response to stress	6.5E-05	
	Individual nodes of interest	GO:2,001,020	Regulation of response to DNA damage stimulus	3.3E-03	
		GO:0006950	Response to stress	1.5E-05	

The table describes in detail the areas influenced by NaBu in Fig. 4A. Clusters characterize the different areas, and each cluster is described by the GO processes supporting the downregulation. For each GO process the description, the number of the proteins and the FDR corrected *q*-value is reported

**Table 4** Downregulated pathways in NaBu-treated CHO DG44-Pr cells

DG44-Pr					
Primary area	Cluster	GO process	Description	FDR <i>q</i> -value	Protein number
Growth arrest	Cellular component biogenesis	GO:0071840	Cellular component organization or biogenesis	2.7E-15	214
		GO:0044260	Cellular macromolecule metabolic process	5.6E-13	185
		GO:0009987	Cellular process	2.8E-10	438
	RNA metabolism	GO:0034661	ncRNA catabolic process	1.0E-03	7
		GO:0090501	RNA phosphodiester bond hydrolysis	2.1E-03	14
		GO:0016073	snRNA metabolic process	2.9E-03	7
		GO:0090503	RNA phosphodiester bond hydrolysis, exonucleolytic	3.0E-02	6
	Ribonucleoprotein complex biogenesis	GO:0034660	ncRNA metabolic process	2.3E-19	56
		GO:0022613	Ribonucleoprotein complex biogenesis	1.5E-14	49
	Cell cycle	GO:0007049	Cell cycle	1.5E-13	79
		GO:0051301	Cell division	6.8E-08	40
	Individual nodes of interest	GO:0051726	Regulation of cell cycle	3.3E-06	55
		GO:0042273	Ribosomal large subunit biogenesis	1.7E-04	13
		GO:1,902,750	Negative regulation of cell cycle G2/m phase transition	3.4E-02	7
DNA replication	Regulation of gene expr, transcription and protein metabolism	GO:0010629	Negative regulation of gene expression	1.2E-08	91
		GO:0051171	Regulation of nitrogen compound metabolic process	2.8E-05	185
		GO:0000122	Negative regulation of transcription by RNA polymerase II	2.9E-03	41
	Peptidyl lysine acetylation	GO:0032268	Regulation of cellular protein metabolic process	1.4E-02	90
		GO:0018205	Peptidyl-lysine modification	3.1E-06	26
		GO:0016569	Covalent chromatin modification	1.4E-05	29
	Mitochondrial gene expression	GO:0018394	Peptidyl-lysine acetylation	8.4E-03	12
		GO:0140053	Mitochondrial gene expression	1.0E-02	10
	DNA replication	GO:0000963	Mitochondrial RNA processing	3.4E-02	4
		GO:0033260	Nuclear DNA replication	3.0E-03	6
Mitosis	DNA conformation change	GO:0006260	DNA replication	5.2E-03	14
		GO:0071103	DNA conformation change	3.9E-04	22
		GO:0006333	Chromatin assembly or disassembly	1.4E-03	16
		GO:0070828	Heterochromatin organization	2.0E-03	9
	Chromatin and chromosome organization	GO:0065004	protein-DNA complex assembly	9.8E-03	14
		GO:0033044	Regulation of chromosome organization	2.2E-06	30
		GO:2,001,251	Negative regulation of chromosome organization	1.1E-02	12
	Spindle assembly	GO:1,902,275	Regulation of chromatin organization	2.7E-02	14
		GO:0032465	Regulation of cytokinesis	1.6E-02	9
		GO:0051255	Spindle midzone assembly	2.9E-02	4
		GO:0000915	Actomyosin contractile ring assembly	2.9E-02	3
	Mitotic nuclear division	GO:0051983	Regulation of chromosome segregation	1.4E-03	12
		GO:0007088	Regulation of mitotic nuclear division	3.2E-03	14
	Individual nodes of interest	GO:0051276	Chromosome organization	1.7E-15	77
		GO:0140014	Mitotic nuclear division	7.6E-08	21
		GO:1,902,850	Microtubule cytoskeleton organization involved in mitosis	5.3E-03	11
GO:0000281		Mitotic cytokinesis	5.5E-03	9	
Stress response	Individual nodes of interest	GO:0033554	Cellular response to stress	2.6E-05	68
		GO:0000012	Single strand break repair	2.9E-02	4
		GO:0080134	Regulation of response to stress	3.1E-02	47

The table describes in detail the areas influenced by NaBu in Fig. 4B. Clusters characterize the different areas, and each cluster is described by the GO processes supporting the downregulation. For each GO process the description, the number of the proteins and the FDR corrected *q*-value is reported

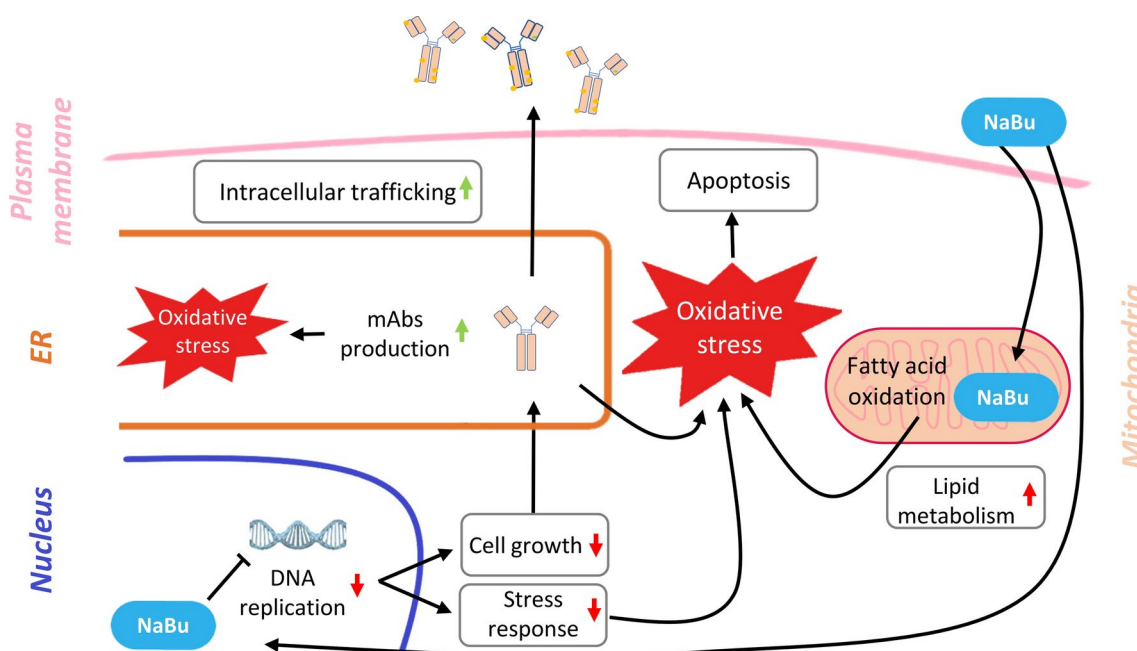


**Fig. 5** Model of butyric acid effect on CHO cells mAbs production. NaBu downregulates the DNA replication affecting the cell growth, which indirectly promotes mAbs production. With a slower growth, cells dedicate resources and machineries to the production and secretion of mAbs, increasing the intracellular trafficking and the oxidative stress deriving from the protein synthesis in the ER. However, the supplemented NaBu is also a fatty acid that has to be oxidized in the mitochondria, resulting in an upregulation of the lipid metabolism of the cells and of the oxidative stress deriving from the mitochondrial activity. The combination of the increased oxidative stress from different sources with the downregulation of the antioxidant response results in an uncontrolled accumulation of oxidative stress in CHO cells, leading to an early apoptosis

## Supplementary Information

The online version contains supplementary material available at <https://doi.org/10.1186/s13568-024-01807-z>.

Additional file 1 (DOCX 905 KB)

## Acknowledgements

We thank all the members of our laboratory, particularly Wang Loo Chien, for the constructive criticisms and the useful suggestions.

## Author contributions

K.S. and C.L. designed and executed the experiments, M.G. performed the proteomics data analysis and drafted the manuscript, Y.K. K.W-K. T.N-K. S.T. X.B. corrected the manuscript, K.W-K. T.N-K. performed the glycan analysis, X.B. conceived and supervised the study and S.T. guided the study. All authors read and approved the final version.

## Funding

The study was financially supported by AB SCIEX Pte Ltd. and Industry Alignment Fund (IAF) from Biomedical Research Council (BMRC) of A\*STAR (Agency for Science, Technology and Research), Singapore (IAF111189).

## Declarations

### Ethics approval and consent to participate

Not applicable.

### Consent for publication

Not applicable.

### Competing interests

All authors declare that they have no competing interest.

## Author details

<sup>1</sup>Bioprocessing Technology Institute (BTI), Agency for Science, Technology and Research (A\*STAR), 20 Biopolis Way, #06-01 Centros, Singapore 138668, Singapore

<sup>2</sup>SCIEX, Concord, ON, Canada

<sup>3</sup>Duke-NUS Medical School, 8 College Rd, Singapore 169857, Singapore

<sup>4</sup>Singapore Institute of Technology, 10 Dover Dr, Singapore 138683, Singapore

Received: 30 November 2024 / Accepted: 6 December 2024

Published online: 24 December 2024

## References

- Al-Rubeai M, Emery AN, Chalder S, Jan DC (1992) Specific monoclonal antibody productivity and the cell cycle-comparisons of batch, continuous and perfusion cultures. *Cytotechnology* 9:85–97. <https://doi.org/10.1007/BF02521735>
- Alsabeeh N, Chausse B, Kakimoto PA, Kowaltowski AJ, Shirihai O (2018) Cell culture models of fatty acid overload: Problems and solutions. *Biochim Biophys Acta Mol Cell Biol Lipids* 1863:143–151. <https://doi.org/10.1016/j.bbalip.2017.11.006>
- Avello V, Torres M, Vergara M, Berrios J, Valdez-Cruz NA, Acevedo C, Molina Sampayo M, Dickson AJ, Altamirano C (2022) Enhanced recombinant protein production in CHO cell continuous cultures under growth-inhibiting conditions is associated with an arrested cell cycle in G1/G0 phase. *PLoS ONE* 17:e0277620. <https://doi.org/10.1371/journal.pone.0277620>
- Bryan HK, Olayanju A, Goldring CE, Park BK (2013) The Nrf2 cell defence pathway: Keap1-dependent and -independent mechanisms of regulation. *Biochem Pharmacol* 85:705–717. <https://doi.org/10.1016/j.bcp.2012.11.016>
- Cabrera G, Cremata JA, Valdés R, García R, González Y, Montesino R, Gómez H, González M (2005) Influence of culture conditions on the N-glycosylation of a monoclonal antibody specific for recombinant hepatitis B surface antigen. *Biotechnol Appl Biochem* 41:67–76. <https://doi.org/10.1042/BA20040032>



- Chng J, Wang T, Nian R, Lau A, Hoi KM, Ho SCL, Gagnon P, Bi X, Yang Y (2015) Cleavage efficient 2A peptides for high level monoclonal antibody expression in CHO cells. *Mabs* 7:403–412. <https://doi.org/10.1080/19420862.2015.1008351>
- Davie JR (2003) Inhibition of histone deacetylase activity by butyrate. *J Nutr* 133:2485S–2493S. <https://doi.org/10.1093/jn/133.7.2485S>
- Dong W, Jia Y, Liu X, Zhang H, Li T, Huang W, Chen X, Wang F, Sun W, Wu H (2017) Sodium butyrate activates NRF2 to ameliorate diabetic nephropathy possibly via inhibition of HDAC. *J Endocrinol* 232:71–83. <https://doi.org/10.1530/JOE-16-0322>
- Dutton RL, Schärer J, Moo-Young M (2006) Cell cycle phase dependent productivity of a recombinant Chinese hamster ovary cell line. *Cytotechnology* 52:55–69. <https://doi.org/10.1007/s10616-006-9041-4>
- Ezquerro S, Becerril S, Tuelo C, Méndez-Giménez L, Mocha F, Moncada R, Valentí V, Cienfuegos JA, Catalán V, Gómez-Ambrosi J, Piper Hanley K, Frühbeck G, Rodríguez A (2020) Role of ghrelin isoforms in the mitigation of hepatic inflammation, mitochondrial dysfunction, and endoplasmic reticulum stress after bariatric surgery in rats. *Int J Obes (Lond)* 44:475–487. <https://doi.org/10.1038/s41366-019-0420-2>
- Gast V, Campbell K, Picazo C, Engqvist M, Siewers V, Molin M (2021) The Yeast eIF2 Kinase Gcn2 Facilitates H2O2-Mediated Feedback Inhibition of Both Protein Synthesis and Endoplasmic Reticulum Oxidative Folding during Recombinant Protein Production. *Appl Environ Microbiol* 87:1–16. <https://doi.org/10.1128/AEM.00301-21>
- Ha TK, Hansen AH, Kol S, Kildegaard HF, Lee GM (2018) Baicalein reduces oxidative stress in CHO cell cultures and improves recombinant antibody productivity. *Biotechnol J*. <https://doi.org/10.1002/Biot.201700425>
- Hague A, Manning AM, Hanlon KA, Hart D, Paraskeva C, Huschtscha LI (1993) Sodium butyrate induces apoptosis in human colonic tumour cell lines in a p53-independent pathway: implications for the possible role of dietary fibre in the prevention of large-bowel cancer. *Int J Cancer* 55:498–505. <https://doi.org/10.1002/IJC.2910550329>
- Han KO, Moon KS, Yang J, Ho CY, Ji SA, Jong ML, Ji TK, Ji UY, Tae HB (2005) Effect of N-Acetylcystein on butyrate-treated Chinese hamster ovary cells to improve the production of recombinant human interferon-beta-1a. *Biotechnol Prog* 21:1154–1164. <https://doi.org/10.1021/BP050057V>
- Hong JK, Lee SM, Kim KY, Lee GM (2014) Effect of sodium butyrate on the assembly, charge variants, and galactosylation of antibody produced in recombinant Chinese hamster ovary cells. *Appl Microbiol Biotechnol* 98:5417–5425. <https://doi.org/10.1007/S00253-014-5596-8>
- Hua J, Xu H, Zhang Y, Ge J, Liu M, Wang Y, Wei Y, Shi Y, Hou LL, Jiang H (2022) Enhancement of recombinant human IL-24 (rhIL-24) protein production from site-specific integrated engineered CHO cells by sodium butyrate treatment. *Bioprocess Biosyst Eng* 45:1979–1991. <https://doi.org/10.1007/S00449-022-02801-0>
- Jiang W, Guo Q, Wu J, Guo B, Wang Y, Zhao S, Lou H, Yu X, Mei X, Wu C, Qiao S, Wu Y (2012) Dual effects of sodium butyrate on hepatocellular carcinoma cells. *Mol Biol Rep* 39:6235–6242. <https://doi.org/10.1007/S11033-011-1443-5>
- Kruh J (1981) Effects of sodium butyrate, a new pharmacological agent, on cells in culture. *Mol Cell Biochem* 42:65–82. <https://doi.org/10.1007/BF00222695/METRICS>
- Lai T, Yang Y, Ng SK (2013) Advances in mammalian cell line development technologies for recombinant protein production. *Pharm* 6:579–603. <https://doi.org/10.3390/PH6050579>
- Lakshmanan M, Kok YJ, Lee AP, Kyriakopoulos S, Lim HL, Teo G, Poh SL, Tang WQ, Hong J, Tan AH-M, Bi X, Ho YS, Zhang P, Ng SK, Lee D-Y (2019) Multi-omics profiling of CHO parental hosts reveals cell line-specific variations in bioprocessing traits. *Biotechnol Bioeng*. <https://doi.org/10.1002/bit.27014>
- Lalonde ME, Durocher Y (2017) Therapeutic glycoprotein production in mammalian cells. *J Biotechnol* 251:128–140. <https://doi.org/10.1016/J.JBIOTEC.2017.04.028>
- Lataster L, Huber HM, Böttcher C, Föller S, Takors R, Radziwill G (2023) Cell cycle control by optogenetically regulated cell cycle inhibitor protein p21. *Biology (Basel)* 12:1194. <https://doi.org/10.3390/BIOLOGY12091194/S1>
- Lee JS, Lee GM (2012) Effect of sodium butyrate on autophagy and apoptosis in Chinese hamster ovary cells. *Biotechnol Prog* 28:349–357. <https://doi.org/10.1002/btpr.1512>
- Li W-F, Fan Z-L, Wang X-Y, Lin Y, Wang T-Y (2022) Combination of sodium butyrate and decitabine promotes transgene expression in CHO cells via apoptosis inhibition. *N Biotechnol* 69:8–17. <https://doi.org/10.1016/j.nbt.2022.02.004>
- Lim Y, Wong NSC, Lee YY, Ku SCY, Wong DCF, Yap MGS (2010) Engineering mammalian cells in bioprocessing—current achievements and future perspectives. *Biotechnol Appl Biochem* 55:175–189. <https://doi.org/10.1042/BA20090363>
- López-Pedrouso M, Borrajo P, Amarowicz R, Lorenzo JM, Franco D (2021) Peptidomic analysis of antioxidant peptides from porcine liver hydrolysates using SWATH-MS. *J Proteomics* 232:104037. <https://doi.org/10.1016/J.JPROT.2020.104037>
- Lu JT, Xiao MK, Feng YY, Wang XY, Le QL, Chai YR, Wang TY, Jia YL (2023) Apilimod enhances specific productivity in recombinant CHO cells through cell cycle arrest and mediation of autophagy. *Biotechnol J* 18:2200147. <https://doi.org/10.1002/Biot.202200147>
- Ludwig C, Gillet L, Rosenberger G, Amon S, Collins BC, Aebersold R (2018) Data-independent acquisition-based SWATH-MS for quantitative proteomics: a tutorial. *Mol Syst Biol* 14:1–23. <https://doi.org/10.15252/msb.20178126>
- Menendez JA, Lupu R (2007) Fatty acid synthase and the lipogenic phenotype in cancer pathogenesis. *Nat Rev Cancer* 7:763–777. <https://doi.org/10.1038/nrc2222>
- Müller B, Heinrich C, Jabs W, Kaspar-Schönefeld S, Schmidt A, Rodrigues de Carvalho N, Albaum SP, Baessmann C, Noll T, Hoffrogge R (2017) Label-free protein quantification of sodium butyrate treated CHO cells by ESI-UHR-TOF-MS. *J Biotechnol* 257:87–98. <https://doi.org/10.1016/J.JBIOTEC.2017.03.032>
- Nakamura H, Matoba S, Iwai-Kanai E, Kimata M, Hoshino A, Nakaoka M, Katamura M, Okawa Y, Ariyoshi M, Mita Y, Ikeda K, Okigaki M, Adachi S, Tanaka H, Takamatsu T, Matsubara H (2012) P53 promotes cardiac dysfunction in diabetic mellitus caused by excessive mitochondrial respiration-mediated reactive oxygen species generation and lipid accumulation/lipid accumulation. *Circ Hear Fail* 5:106–115. <https://doi.org/10.1161/CIRCHEARTFAILURE.111.961565>
- Newcombe AR (2014) The Evolution of quality by design (QbD) for biologics. *PDA J Pharm Sci Technol* 68:320–322. <https://doi.org/10.5731/PDAJ.PST.2014.00989>
- Nguyen P, Leray V, Diez M, Serisier S, Bloc H, Le J, Siliart B, Dumon H (2008) Liver lipid metabolism. *J Anim Physiol Anim Nutr (Berl)* 92:272–283. <https://doi.org/10.1111/j.1439-0396.2007.00752.x>
- Orellana CA, Marcellin E, Gray PP, Nielsen LK (2017) Overexpression of the regulatory subunit of glutamate-cysteine ligase enhances monoclonal antibody production in CHO cells. *Biotechnol Bioeng* 114:1825–1836. <https://doi.org/10.1002/Biot.26316>
- Ortiz-Enriquez C, de Romero-Díaz AJ, Hernández-Moreno AV, Cueto-Rojas HF, Miranda-Hernández MP, López-Morales CA, Pérez NO, Salazar-Ceballos R, Cruz-García N, Flores-Ortiz LF, Medina-Rivero E (2016) Optimization of a recombinant human growth hormone purification process using quality by design. *Prep Biochem Biotechnol* 46:815–821. <https://doi.org/10.1080/10826068.2015.1135467>
- Ozcan U, Cao Q, Yilmaz E, Lee A-H, Iwakoshi NN, Ozdelen E, Tuncman G, Gorgun C, Glimcher LH, Hotamisligil GS (2004) Endoplasmic reticulum stress links obesity, insulin action, and type 2 diabetes. *Science* 306:457–461. <https://doi.org/10.1126/science.1103160>
- Park SY, Egan S, Cura AJ, Aron KL, Xu X, Zheng M, Borys M, Ghose S, Li Z, Lee K (2021) Untargeted proteomics reveals upregulation of stress response pathways during CHO-based monoclonal antibody manufacturing process leading to disulfide bond reduction. *Mabs*. <https://doi.org/10.1080/19420862.2021.1963094>
- Rios-Morales M, Vieira-Lara MA, Homan E, Langelaar-Makkinje M, Gerding A, Li Z, Huijkmans N, Rensen PCN, Wolters JC, Reijngoud DJ, Bakker BM (2022) Butyrate oxidation attenuates the butyrate-induced improvement of insulin sensitivity in myotubes. *Biochim Biophys Acta - Mol Basis Dis* 1868:166476. <https://doi.org/10.1016/J.BBADIS.2022.166476>
- Rizzo D, Cerofolini L, Giuntini S, Iozzino L, Pergola C, Sacco F, Palmese A, Ravera E, Luchinat C, Baroni F, Fragai M (2022) Epitope mapping and binding assessment by solid-state nmr provide a way for the development of biologics under the quality by design paradigm. *J Am Chem Soc* 144:10006–10016. [https://doi.org/10.1021/JACS.2C03232/SUPPL\\_FILE/JA2C03232\\_SI\\_001.PDF](https://doi.org/10.1021/JACS.2C03232/SUPPL_FILE/JA2C03232_SI_001.PDF)
- Rodríguez J, Spearman M, Huzel N, Butler M (2005) Enhanced production of monomeric interferon-beta by CHO cells through the control of culture conditions. *Biotechnol Prog* 21:22–30. <https://doi.org/10.1021/BP049807B>
- Salimi V, Shahsavari Z, Safzadeh B, Hosseini A, Khademi N, Tavakoli-Yaraki M (2017) Sodium butyrate promotes apoptosis in breast cancer cells through reactive oxygen species (ROS) formation and mitochondrial impairment. *Lipids Health Dis* 16:1–11. <https://doi.org/10.1186/S12944-017-0593-4/FIGURE5>
- Schubert OT, Gillet LC, Collins BC, Navarro P, Rosenberger G, Wolksi WE, Lam H, Amodè D, Mallick P, Maclean B, Aebersold R (2015) Building high-quality assay libraries for targeted analysis of SWATH MS data. *Nat Protoc* 10:426–441. <https://doi.org/10.1038/nprot.2015.015>
- Schulze M, Kumar Y, Rattay M, Niemann J, Wijffels RH, Martens DE (2022) Transcriptomic analysis reveals mode of action of butyric acid supplementation in an

- intensified CHO cell fed-batch process. *Biotechnol Bioeng* 119:2359–2373. <https://doi.org/10.1002/BIT.28150>
- Semaan J, El-Hakim S, Ibrahim JN, Safi R, Elnar AA, El Boustany C (2020) Comparative effect of sodium butyrate and sodium propionate on proliferation, cell cycle and apoptosis in human breast cancer cells MCF-7. *Breast Cancer* 27:696–705. <https://doi.org/10.1007/S12282-020-01063-6>
- Senior M (2023) Fresh from the biotech pipeline: fewer approvals, but biologics gain share. *Nat Biotechnol* 41:174–182. <https://doi.org/10.1038/s41587-022-01630-6>
- Sim KH, Liu LCY, Tan HT, Tan K, Ng D, Zhang W, Yang Y, Tate S, Bi X (2020) A comprehensive CHO SWATH-MS spectral library for robust quantitative profiling of 10,000 proteins. *Sci Data*. <https://doi.org/10.1038/S41597-020-00594-Z>
- van Eunen K, Simons SMJ, Gerding A, Bleeker A, den Besten G, Touw CML, Houten SM, Groen BK, Krab K, Reijngoud DJ, Bakker BM (2013) Biochemical competition makes fatty-acid  $\beta$ -oxidation vulnerable to substrate overload. *PLoS Comput Biol*. <https://doi.org/10.1371/journal.pcbi.1003186>
- Walker DE, Yang F, Carver J, Joe K, Michels DA, Yu XC (2017) A modular and adaptive mass spectrometry-based platform for support of bioprocess development toward optimal host cell protein clearance. *Mabs* 9:654. <https://doi.org/10.1080/19420862.2017.1303023>
- Walther TC, Farese RV (2012) Lipid droplets and cellular lipid metabolism. *Annu Rev Biochem* 81:687. <https://doi.org/10.1146/ANNUREV-BIOCHEM-061009-102430>
- Wang CH, Wang CC, Huang HC, Wei YH (2013) Mitochondrial dysfunction leads to impairment of insulin sensitivity and adiponectin secretion in adipocytes. *FEBS J* 280:1039–1050. <https://doi.org/10.1111/febs.12096>
- Wippermann A, Rupp O, Brinkrolf K, Hoffrogge R, Noll T (2017) Integrative analysis of DNA methylation and gene expression in butyrate-treated CHO cells. *J Biotechnol* 257:150–161. <https://doi.org/10.1016/J.JBIOTECH.2016.11.020>

### Publisher's Note

Springer Nature remains neutral with regard to jurisdictional claims in published maps and institutional affiliations.